Article

Assessment of Run-Off Waters Resulting from Lithium-Ion Battery Fire-Fighting Operations

Arnaud Bordes [ID], Arnaud Papin, Guy Marlair *[ID], Théo Claude, Ahmad El-Masri, Thierry Durussel, Jean-Pierre Bertrand, Benjamin Truchot [ID] and Amandine Lecocq

Institut National de l'Environnement Industriel et des Risques (Ineris), Parc Technologique Alata, BP2, 60550 Verneuil-en-Halatte, France; arnaud.bordes@ineris.fr (A.B.); arnaud.papin@ineris.fr (A.P.); ahmad.el-masri@ineris.fr (A.E.-M.); benjamin.truchot@ineris.fr (B.T.)
* Correspondence: guy.marlair@ineris.fr; Tel.: +33-344556348

Abstract: As the use of Li-ion batteries is spreading, incidents in large energy storage systems (stationary storage containers, etc.) or in large-scale cell and battery storages (warehouses, recyclers, etc.), often leading to fire, are occurring on a regular basis. Water remains one of the most efficient fire extinguishing agents for tackling such battery incidents, and large quantities are usually necessary. Since batteries contain various potentially harmful components (metals and their oxides or salts, solvents, etc.) and thermal-runaway-induced battery incidents are accompanied by complex and potentially multistage fume emissions (containing both gas and particles), the potential impact of fire run-off waters on the environment should be considered and assessed carefully. The tests presented in this paper focus on analyzing the composition of run-off waters used to spray NMC Li-ion modules under thermal runaway. It highlights that waters used for firefighting are susceptible to containing many metals, including Ni, Mn, Co, Li and Al, mixed with other carbonaceous species (soot, tarballs) and sometimes undecomposed solvents used in the electrolyte. Extrapolation of pollutant concentrations compared with PNEC values showed that, for large-scale incidents, run-off water could be potentially hazardous to the environment.

Keywords: Li-ion battery; fire; safety; thermal runaway; toxicity; water; firefighting; pollutants

1. Introduction

The current development of Li-Ion batteries concerns numerous, application fields, and the thermal runaway hazard about those systems, often leading to fire and sometimes explosion events, remains a resilient issue. In parallel to the wide spread of Li-ion-powered consumer products in complex built environments, the increasing use of applications of LIB for e-mobility or large-scale battery energy storage systems (BESS), in the hundreds of MW power range, requires the urgent development of environmentally friendly strategies to fight lithium-ion battery fires. Considering that water remains one of the most efficient fire extinguishing agents to fight battery fires, and in many cases is the only extinguishing medium available in operational quantities to the fire-brigades, the potential impact of relating fire run-off waters to the environment should be considered and assessed carefully. Lessons of the past have primarily shown that uncontrolled release of toxic fire waters in rivers may lead to a dramatic consequence for water livestock, as primarily shown by major incidents involving large storage of toxic chemicals such as in Basle (Sandoz fire, Switzerland, 1986) [1,2] or in Tianjin (China, 2015) [3]. This is a prerequisite for establishing a clear and science-based firewater management doctrine [4]. In particular, the level of contamination of fire waters in terms of toxicity to aquatic ecosystems is needed to decide on the free release of extinguishing waters into the environment or into rainwater drain systems or on their containment in suitable systems for post-hazardous liquid waste management [5].

During the thermal runaway phenomenon—initiating stage of relating field failures—it is well-known that systems containing Li-ion batteries produce emissions or effluents which can range anywhere within the full spectrum of physical states, e.g., liquids (electrolyte leak or ejection), gases or vapors or solid aerosols [6–10], which adds complexity to both non-flaming and flaming conditions. These emissions may in turn interact with the environment and lead to pollution [11]. One of the contamination modes of both land and aquatic ecosystems is the aerosol sedimentation process arising during smoke plume dispersion, often at a stage where contaminant concentrations in the smoke plume are significantly diluted at a certain distance from the incident. Another possible and easier way of pollution is linked to the extinguishing agents used, typically water used by fire suppression systems or fire brigades, which can carry effluents emanating from the damaged battery. These various modes of contamination have been, unfortunately, largely confirmed in a significant number of fire records, as exemplified by Mc Namee et al. [12]. This shows, in particular, the diversity of influencing factors in terms of burning materials, size, and fire duration, potentially leading to environmental damage. Regarding batteries, the contaminants involved depend on the materials composing the system. These materials vary from one Li-ion battery chemistry/geometry to another and from one system to another, but the phenomena at stake and the resulting effects are close [13]. For small- or medium-isolated batteries (e.g., used for portable applications), the accidental contamination risk should be relatively low, but for more energy- or power-demanding applications leading to larger battery systems (containerized BESS, ...) or large-scale cell and battery storages (warehouse, recyclers, ...), the consequences might start to raise concerns in the absence—so far the usual case—of any fire water containment capacity. As a matter of fact, according to EPRI information, 64% of the BESS site owners are considering the implementation of water containment for the firefighting run-off waters [4]. Regarding fire extinguishing waters used to tackle car fires, if detailed studies [14,15] of fire water ecotoxicity had concluded that subsequent fire water run-off had a negligeable impact on the environment, as far as ICE cars are concerned, more caution is likely to be needed with EVs, given the significant differences applied from potential contaminants from the battery and the amount of water requirements.

Emissions during thermal events are directly linked to the materials constituting the battery. However, they will possibly be altered by reactions of thermal decomposition, electrolysis or even combustion that might drastically change the nature and properties of the ejected matter [8]. Carrying those substances by water will vary depending on the chosen extinguishing method. Three options are generally possible: (1) Direct watering of the batteries—when sprinklers or water fire hose are directed to the faulty system with direct contact with the batteries. (2) Fire plume watering for fire and smoke progress abatement—when water is not applied directly to the system but to its surroundings to prevent fire and subsequent damage propagation to adjacent elements and therefore minimize the impact of the root fire. (3) Water immersion—when the battery is immersed in a large volume of water, either after an incident to cool down the sample, or during an incident to try to limit it. In this last option, managing firefighting waters is relatively simple as water is already contained.

Water contamination in the smoke watering scenario (#2 firefighting option) was recently studied by EMPA [16,17] while analysis of immersion water (#3 firefighting option) has been performed both by EMPA and RIVM [18]. However, more globally, published information regarding contamination of fire waters used to tackle li-ion battery fires, regardless of the application, remains quite scarce. Therefore, further investigation is needed to confirm the early trends observed [19] and to address those issues in the entire value chain of LIBs.

In the present paper, the case of direct watering of the batteries is the only scenario studied. Commercially available NMC battery modules composed of two different cell formats (18,650 and prismatic) were chosen for the experimental approach selected in this study.

2. Materials and Methods

2.1. Description of the Samples

Two types of commercial Li-ion modules were used, both composed of NMC/graphite cells.

Module A comprises 16-metal-can prismatic cells (7.5 Ah) and has an electrical energy of 500 Wh. In addition to the electrochemical cells, the module also includes metallic (aluminum plates, cells connectors) and plastic (casing cover, wire insulation etc.) parts.

Module B is an assembly of 2 cell blocks, each one composed of 45-cylindrical 18,650 cells (2.4 Ah), circled with a metallic grid to ensure its mechanical integrity. The total energy of the battery assembly is 900 Wh. In addition to the electrochemical cells, the module also integrates a thin plastic film keeping the cells tightly together and connected.

The week before the abuse tests, the modules were fully charged using a constant current profile at C/5 using a cycling bay from FEV manufacturer.

2.2. Abuse Tests Set Up

Abuse tests on modules were performed in the Ineris 80 m^3 test chamber equipped with a smoke exhaust and treatment system remotely controlled to fully extract, measure, and eventually convey gases through the gas cleaning system of the facility before their rejection to the atmosphere. The room is also connected to a water-draining system to collect all liquid effluents produced by the fire or during the fire suppression process. In the testing room, the air entrance is located on one side, near the ground; extraction is placed in the center of the roof. All tests were performed under air with an extraction flow rate in the test chamber of approximately 2 500 m^3/h.

The sample was positioned in the center of the test chamber for each test, as represented in Figure 1. Modules were positioned on a metal grid, electrically insulated, using a small support made of inert material (calcium silicate).
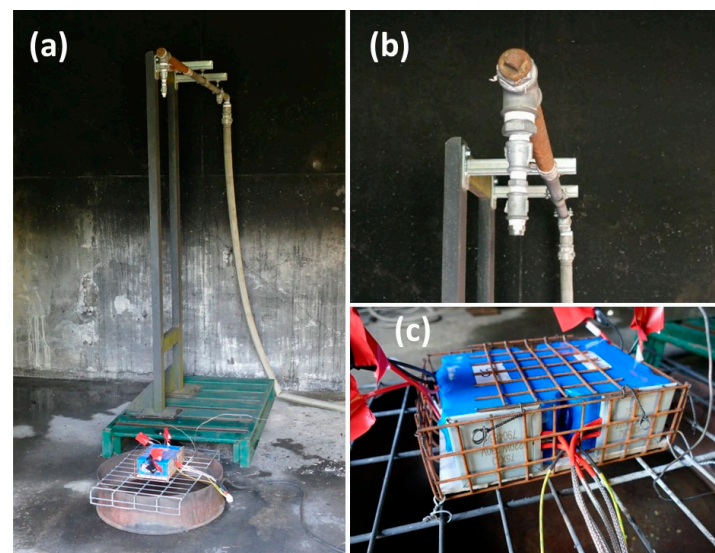
Figure 1. Pictures of the experimental set-up. (**a**) Overview, (**b**) sprinkler head, and (**c**) battery module B. White pads on the front faces of each battery block correspond to the heaters.

For module A, as the thermal pad failed to initiate a thermal runaway, a 20 kW gas burner was selected and positioned 30 cm from the sample and directed to the middle of the module. To prevent any interaction between the propane burner and the water used for firefighting, the burner was switched off as soon as thermal runaway was triggered.

For module B, two thermal pads with individual power of 220 W and a 50 cm^2 surface were put in contact with each cell block.

Since the objective of the tests was to evaluate water contamination in thermal runaway situations, the sprinkler activation was performed manually as soon as the thermal runaway was visually confirmed. As the modules were not equipped with thermocouples, the thermal runaway event was considered occurring when flames were escaping for the first time from the module. The application rate was set at 10 L/m^2/min. The basin surface was 0.25 m^2, and the volume of collected water was estimated by calculation using the water flow, the watering time, and the basin surface.

2.3. Water Sampling

After each test, 2 L of water was immediately sampled from the extinguishing water containment basin for chemical composition analysis. It is important to highlight that no filtration was made to keep all of the emissions in the analyzed samples, whatever the chemical or physical processes that were involved in the interactions of emissions from the battery module and extinguishing waters (condensation, dissolution, sedimentation etc.), since the objective of the test was to characterize the global composition of runoff water.

Before the test, the water receptacle was exposed to a direct flame to remove the potential traces of organic solvents. However, deposit remains possible, and a reference was then carried out by watering the same set-up, without any battery, in order to have a baseline of potential species inherently present in the water supply or due to receptacle component extraction during sampling.

2.4. Water Analysis

2.4.1. Inductively Couple Plasma Optical Emission Spectroscopy

Inductively Couple Plasma Optical Emission Spectroscopy (ICP-OES, Agilent 5110 equipment, Santa Clara, CA, USA) has been used for the analysis of major elements (Al, Fe, Li, Na, Ni, P).

2.4.2. Inductively Couple Plasma Mass Spectrometry

Inductively Couple Plasma Mass Spectrometry (ICP-MS, Agilent 7900 instrument, Santa Clara, CA, USA) has been used for the analysis of trace elements (Co, Cu, Mn). Instead of the ICP-OES used for major elements by measuring the light emitted from elements, ICP-MS uses a quadrupole to filter the ions according to their mass/charge ratio and counts each mass passed to the detector. The high sensitivity of the ICP-MS detector provides a much lower detection limit than ICP-OES.

2.4.3. Ion Chromatography

Chloride and fluoride species were measured by ion chromatography (Metrohm, 850 Professional IC, Herisau, Switzerland) with conductimetric detection. Ion chromatography is a method for separating ions (Cl^- and F^-) based upon their interactions with resin (stationary phase) and the eluent (mobile phase).

2.4.4. Liquid Chromatography

To extract polycyclic aromatic hydrocarbons (PAHs) from the water sample, a separation of the particle phase was carried out using glass wool. Aqueous phases were extracted using dichloromethane by liquid/liquid extraction and particulate phase was extracted using acetonitrile. Both extracts were evaporated and collected in 0.5 mL of acetonitrile each and recombined in the same vial before analysis.

Analysis of PAHs was performed on a liquid chromatography system, an ultimate 3000 from thermo coupled to a diode array detector (DAD) and fluorescence detector (FLD) detector. Molecules were separated on C18 column (Zorbax eclipse PAH 2.1 × 150 mm 1.8 micron from Agilent). All PAHs were quantified using the FLD detector except for Acenaphthylene that was quantified using the UV-DAD detector.

2.4.5. Gas Chromatography

Carbonates were analyzed using a gas chromatography system from Varian. Samples were diluted in methanol and 1µL was injected in split mode 1:10. Separation was performed on a capillary column from Agilent VF-5 ms 60 m, 0.25 mm internal diameter and 1 µm film thickness. A flame ionization detector was used to quantify the different compounds.

2.5. Particle Morphology Characterization

A particle size distribution analysis using the centrifugal disc method (by use of CPS Disc Centrifuge™ instrument, Tokyo, Japan) and further particle morphology study by Transmission Electron Microscopy (TEM, JEOL 1400 Plus instrument, Tokyo, Japan) were carried out on the sampled water. To enable this analysis, all particles larger than 2 µm in size were filtered beforehand.

To perform microscopic analysis of the particles, a droplet of the sample suspension was casted on a copper grid and dried at room temperature to be observed with a TEM (Transmission Electron Microscope, JEOL, 1400 Plus, Tokyo, Japan). A beam of electrons accelerated by a high voltage (120 kV) passes through a very thin sample, in this case a carbonized copper grid on which a microdrop of the sample to be analyzed was deposited. During the electron–matter interaction, the transmitted and diffracted electrons are used to form an image with high resolution in gray levels, and the X-ray photons allow for a micro or even a nano-volume of the sample to be chemically characterized.

## 3. Results

3.1. Test Conditions and TR Characteristics

Table 1 compiles the test conditions and reactions observed during the three successive test runs and Figure 2 gives details on the timeline of the experiments and presents pictures of the markers of significant events.

Table 1. Summary of test conditions and observations.

	Module Type	Module Energy	Heating Method	Reaction	Module State after Test	Sprinkler Flow	Amount of Water Delivered
Test 1	Prismatic cell assembly NMC (module A)	500 Wh	Gas burner	Venting + moderate fire	Upper plastic burnt Mechanical integrity conserved No module casing opening	10 $L/m^2/min$	7 L
Test 2	Prismatic cell assembly NMC (module A)	500 Wh	Gas burner	Jet fire + explosion	Module casing ejected All cells fully burnt with casing damaged	10 $L/m^2/min$	7 L
Test 3	Cylindrical cell assembly NMC (module B)	900 Wh	Thermal pad	Jet fire + explosion	All cells burnt Some jelly rolls visible	10 $L/m^2/min$	9 L

In the first experiment, the thermal runaway of module A was characterized by the emission of a large amount of white smoke followed by the appearance of flames. No jet fire was observed, but a rather moderate combustion process, as visible on the first line of Figure 2 was observed. Water was applied for 2 min 50 s, corresponding to a volume of collected water of 7 L. The flames stopped as soon as water was applied. After the test, no cells presented any side wall rupture, and their mechanical integrity was conserved.
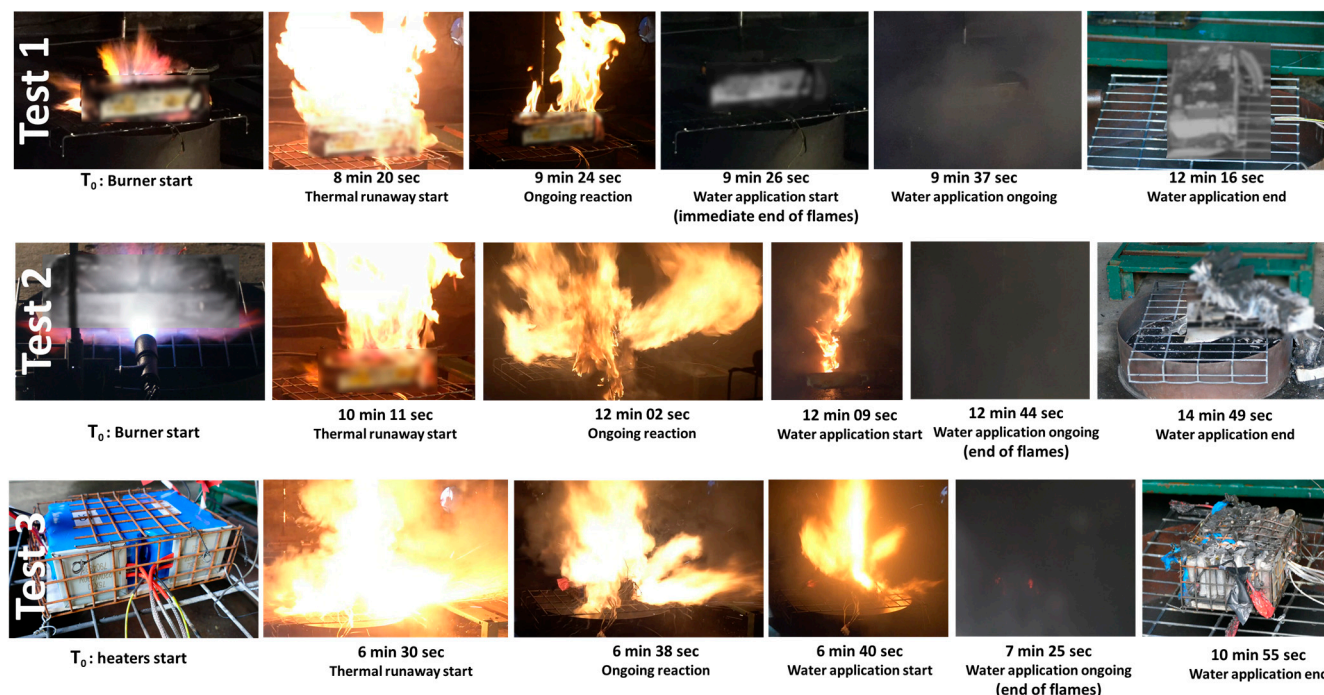
Figure 2. Extracts from the test video and timeline of the three experiments.

Test 2 was performed because module A was only moderately impacted by the first experiment. It was decided that the thermal runaway of module A should be further pushed and to restart the burner. After a few minutes of heating, the module entered again in the thermal runaway process. In this case, the reaction was much more violent since the jet fire was observed, the module casing was ejected, and all cells subsequently seemed damaged, some of them losing their mechanical integrity (casing opening). The second line of Figure 2 shows the reaction's visible effects just before water application (12 min 9 s). Water was applied for 2 min 40 s, leading to an additional volume of collected water of 7 L, i.e., a total of 12 L considering 5 L remains from test 1 (after that 2 L were sampled for analysis). Contamination levels indicated for test 2 are the values corresponding to the mix of the 5 L remaining from test 1 and the 7 L applied during test 2. The flames did not stop immediately upon water application, and an unknown portion of the water vaporized before reaching the receptacle. In the first approximation, this proportion of water vaporized was not considered for further calculation of the contaminant. The flames stopped 35 s after the application of water.

For module B, a single TR/fire water suppression step was carried out when the thermal runaway was reached. The third line of Figure 2 shows that the reaction was rather violent. All of the cells seemed damaged after the test and some of them lost their mechanical integrity (casing opening or jelly roll ejection). Water was applied for 3 min 30 s corresponding to a volume of collected water of 9 L, neglecting once more the vaporizer part. Flames stopped 45 s after water activation.

3.2. Characterization of Water Contamination

3.2.1. Halogens and Metals

Table 2 shows the results of the analyses for the presence of the two anions (F^- and Cl^-) as well as a selection of metal compounds. Those species have been chosen to reflect the foreseeable pollutants considering NMC Li-ion batteries composition [20].

As expected, the levels of fluorides and metals are found in large amounts, due to the composition of the cells. In module A, phosphorus and fluoride ions are the dominant species. In contrast, in module B, lithium is the more concentrated pollutant element compared to all other metallic elements and fluorides or chlorides. All these species are

found in cell electrolytes or in the electrode for Li. Transition metals contained in the cathode (Ni, Mn, Co) are found mainly when the reaction was violent (tests 2 and 3). Their ratios, across different tests vary but in the three tests, Ni is overrepresented compared with Mn and Co, which is expected as stoichiometry of the current NMC cathode favors Ni. Their presence—in undetermined metal containing chemicals (oxides ? hydroxides ? metal complexes ?) [21]—is consistent, with composition of the selected cells. In order to better understand their respective amount, further studies on their chemical state and their solubility in water are necessary.

Table 2. Analysis of anions (F^- and Cl^-) and a selection of metals in the water before application and in the three samples after extinguishing. QL = quantification limit. Uncertainty values refer to expanded uncertainties (k = 2).

	QL	Uncertainty	Reference	Test 1 (Module A)	Test 2 (Module A)	Test 3 (Module B)
			Ions			
F^- (mg/L)	0.05	8%	0.25	142	91.6	93.7
Cl^- (mg/L)	0.01	3%	24.9	33.4	36.5	203
			Metals			
Al (mg/L)	0.17	15%	0.91	74.2	29.3	73.9
Co (mg/L)	0.03	10%	<LQ	0.42	12.8	7.07
Cu (mg/L)	0.03	10%	0.04	0.30	0.26	4.18
Fe (mg/L)	0.08	9%	0.30	5.92	4.59	0.30
Li (mg/L)	1.67	15%	<LQ	44.5	27.8	360
Mn (mg/L)	0.03	10%	<LQ	1.22	17.0	5.82
Na (mg/L)	1.67	14%	13.0	15.6	16.3	26.2
Ni (mg/L)	0.08	12%	<LQ	3.25	49.0	40.1
P (mg/L)	0.17	17%	<LQ	201	113	5.80

Aluminum, copper, and iron in pristine cells are present in sheets or bulk form and as particulate matter; therefore, they are expected to be less present in particulate emission. Aluminum is, however, found in noteworthy amounts probably because of its low melting point (660 °C). Iron and copper, which have higher melting points are found in relatively low amounts in the three tests.

By comparing the two extinguishing operations on the prismatic cells (test 1 and 2), it can be observed that when the thermal runaway thermal impact is characterized by a fully developed combustion process, the interacting water collected is much more concentrated in Polycyclic Aromatic Hydrocarbon (PAHs) and cathode metals (Ni, Mn, Co). On the other hand, the concentrations of elements essentially coming from the liquid electrolyte (typically Li, P, F) are present in higher quantities (1.6 to 1.8 factor) when the reaction is not fully developed, and where the electrolyte has a chance to be dragged in the water. This observation is coherent with the higher amount of organic carbonates found in test 1 presented in Section 3.2.3.

The comparison of the results between different cell geometries also confirms the importance of this parameter, influencing, in particular, the mechanical strength of the system and, therefore, the confinement of the species.

3.2.2. Poly Aromatic Hydrocarbons (PAHs)

Another important family of water contaminants in fire situations is PAHs. While the common specification for PAHs mentions 16 substances to be analyzed [22], 23 PAHs were analyzed; the results are reported in Table 3.

Table 3. Analysis of 23 PAHs in the water before application and in the three samples after extinguishing. QL = quantification limit. (Expanded: k = 2) Uncertainty of analysis for HAPs is 15% for all species.

PAH (Polycyclic Aromatic Hydrocarbons)					
	QL	Reference	Test 1 (Module A)	Test 2 (Module A)	Test 3 (Module B)
Naphtalène (ng/L)	10.0	<LQ	1279.2	2792.2	3114.6
Acénaphtylène (ng/L)	40.0	<LQ	2421.7	2405.1	1193.4
méthyl-1.naphtalène (ng/L)	10.0	<LQ	26.8	459.4	667.1
méthyl-2.naphtalène (ng/L)	10.0	<LQ	203.2	<LQ	2058.4
Acénaphtène (ng/L)	2.0	<LQ	34.1	110.6	275.7
Fluorene (ng/L)	2.0	<LQ	74.1	752.3	1055.0
Phénanthrène (ng/L)	4.0	5.7	360.9	3026.8	2581.6
Anthracène (ng/L)	2.0	<LQ	10.6	330.5	303.3
Fluoranthène (ng/L)	2.0	10.8	57.7	1280.9	349.8
Pyrène (ng/L)	2.0	7.2	45.1	1279.8	20.5
méthyl-2.fluoranthène (ng/L)	4.0	<LQ	7.3	45.1	21.3
B(a)A (ng/L)	2.0	<LQ	24.8	185.7	131.8
Chrysene (ng/L)	2.0	<LQ	32.5	212.3	40.8
Retene (ng/L)	2.0	<LQ	104.9	170.7	19.8
B(e)P (ng/L)	2.0	<LQ	7.5	306.3	50.4
B(j)F (ng/L)	20.0	<LQ	<LQ	106.3	<LQ
B(b)F (ng/L)	2.0	<LQ	34.6	259.6	5.8
B(k)F (ng/L)	2.0	<LQ	8.3	81.0	8.2
B(a)P (ng/L)	2.0	<LQ	13.0	163.9	20.8
D(a.h)A (ng/L)	2.0	<LQ	<LQ	36.7	4.5
benzo(ghi)P (ng/L)	2.0	<LQ	13.3	169.6	4.1
Indèno (ng/L)	4.0	<LQ	35.2	162.1	11.8
Coronene (ng/L)	2.0	<LQ	4.0	54.0	<LQ

It shows the presence of numerous PAHs including naphtalene and phenantrene, the most present, which typically indicates the combustion of hydrocarbon-based products. Specific attention should be paid to B(a)P as it is class 1 on the IARC scale (proven carcinogen). According to the potential ecotoxicological impact of those products, one should pay specific attention to the potential impact of runoff water.

3.2.3. Organic Carbonates

To complete the chemical characterization of the pollutants in the extinguishing waters, a selection of organic carbonates, classically used as electrolyte solvents or critical additives (VC, FEC), was quantified. Results are shown in Table 4.

Table 4. Analysis of 7 common carbonates used as electrolytes in the water before application and in the three samples after extinguishing. QL = quantification limit.

| Species	QL	Reference	Test 1 (Module A)	Test 2 (Module A)	Test 3 (Module B)
DMC (µg/mL)	8.8	n/a	n/a	n/a	n/a
EMC (µg/mL)	8.3	n/a	138	59	n/a
VC (µg/mL)	9.4	n/a	n/a	n/a	n/a
DEC (µg/mL)	8.1	n/a	n/a	n/a	n/a
FEC (µg/mL)	10.2	n/a	n/a	n/a	n/a
EC (µg/mL)	7.7	n/a	1082	461	n/a
PC (µg/mL)	10	n/a	n/a	n/a	n/a

The presence of such compounds is found only in tests 1 and 2. This difference between the tests could be explained by the important combustion reaction observed during tests 3; it

is most likely that the high temperature reached during this test led to the total evaporation and possible thermal decomposition of those volatile and easily flammable compounds before being dragged into the wastewaters. The boiling point for EC is typically 244 °C and 100 °C for EMC, which is significantly lower than the flame temperature. For the same reason, as the reaction in test 1 was less violent than in test 2, the quantity of carbonates found is higher for test 1 than for test 2. Species identified in the water are EMC and EC which are very commonly used as electrolyte solvents. Also, the boiling point difference might explain the difference between the quantity of EC and EMC found in the liquid phase, as EMC evaporates more easily. This also means that the massive use of water to cool down a whole system as a container could lead to a higher concentration of organic carbonates since part of the cells might, in such a case, be damaged but not burnt. Hydro solubility of those compounds may also play an important role (778 g/L for EC and 46.8 g/L at 20 °C for EMC) and explain the differences in the concentrations found. These compounds must be carefully monitored because they cannot easily be filtered out or left to settle.

3.2.4. Particle Size Analysis

To complete the chemical analysis of the water, particles sizes in the water were evaluated using the CPS method. Using Stokes' law, a hydrodynamic intensity-weighted particle-size distribution of diameters is obtained and transformed into a volume-weighted or number-weighted particle-size distribution, as presented in Figure 3.
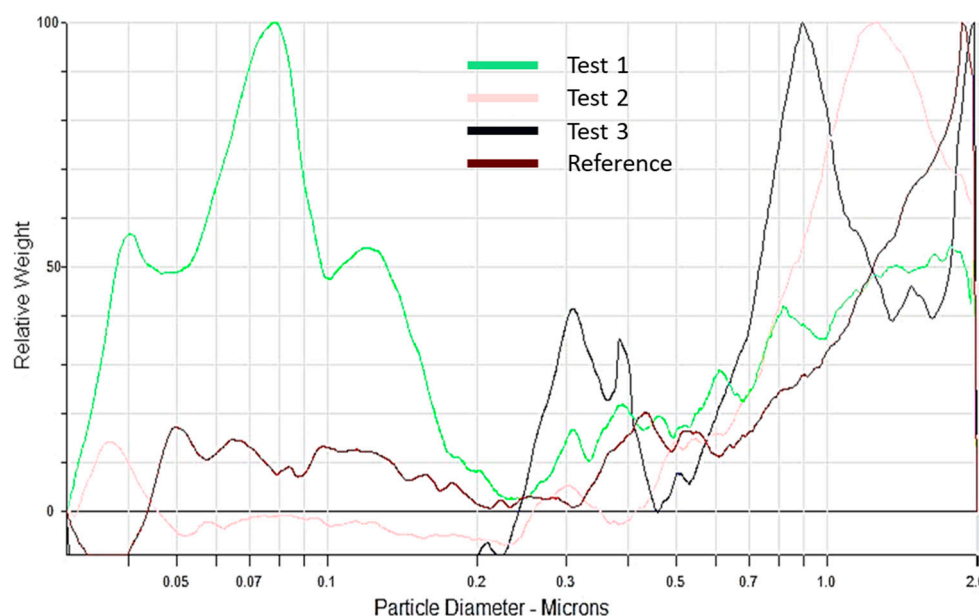

Figure 3. Number-weighted particle-size distribution of the particles presents in the water before application (reference) and in the three samples after extinguishing. Measurement was carried out by CPS.

This analysis leads to the conclusion that only extinguishing water from test 1 has a nanometric fraction, with particles around 70 nm in diameter. Other samples contain a majority of particles between 0.9 and 2 µm. This analysis confirms the possibility, mentioned in the literature [11], that extinguishing water might be loaded with nanoparticles, without being able to quantify them with the method used. Also, because nanoparticles are absent from tests where the reaction was the most developed, it can indicate that those particles might be dragged in the smoke plume before being dragged by water.

To get information on the nature of the nanometric particles in the extinguishing water of test 1, additional analysis by transmission electron microscopy were performed. Images are presented in Figure 4. Figure 4a shows a picture of a representative sample of what was observed over the entire grid. Several populations of particles of highly variable sizes

are identified and presented on Figure 4b–d. The majority of particles are the finest and correspond to the smallest black dots in Figure 4a. According to Figure 4b, one can conclude that soot nanoparticles agglomerate and form nanostructured clusters. Spherical particles of intermediate size are then observed (Figure 4c) and are associated with tarballs, having a diameter around 100 nm. Finally, the largest particles (Figure 4d) have a characteristic size around one micron and are mainly metal particles, composed of iron and aluminum.
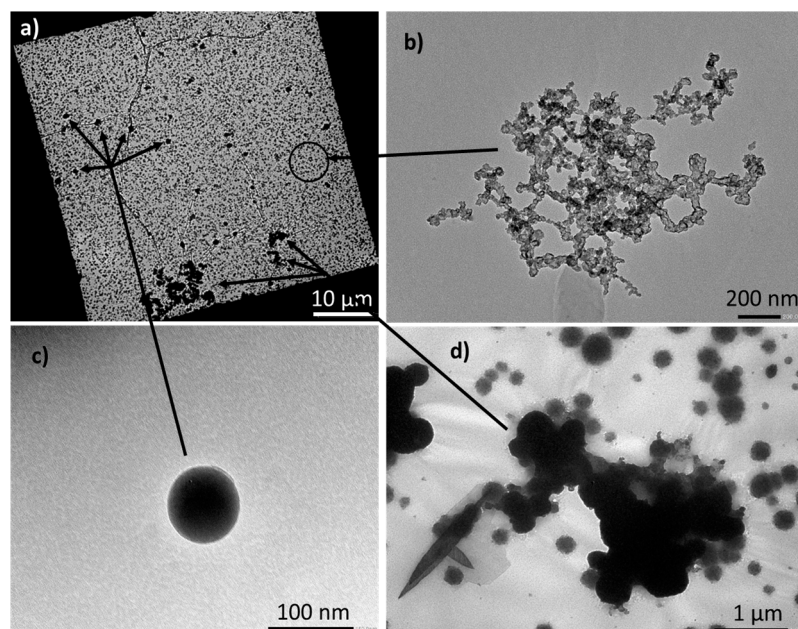
Figure 4. TEM analysis of the particles presents in the extinguished water of test 1. (**a**) Zoom-out of a representative area showing the relatives proportion of the three particles population encountered, (**b**) zoom-in of particles identified as soot agglomerate, (**c**) zoom-in of particles identified as tarballs and (**d**) zoom-in of particles identified as metallic.

Particles bellow 2.5 μm are inhalable and might pose a toxicological risk for humans [23]. In the case of this study, the particles are in water, making eco-toxicity the main risk identified. No size threshold is clearly defined in the literature nor in regulations. Some studies have nonetheless showed that particles with a size lower than 100 nm can enter the root system of higher plants and be translocated to aerial parts which demonstrate the possibility of trophic transfer [24]. In invertebrates (water flee), accumulation of several types of nanomaterials has been shown [25]. The interaction phenomenon between metallic oxide nano materials and freshwater micro-algae was also evidenced by Rivero et al. [26].

3.2.4.1. pH Measurement

Table 5 shows the pH measured in the sampled water immediately after each test.

Table 5. pH of the extinguishing water. (Expanded: k = 2) uncertainty of measurement is 1%.

	Test 1 (Module A)	Test 2 (Module A)	Test 3 (Module B)
pH	5.2	5.9	11

Depending on the test, the pH of extinguishing water is either acidic or basic. Values obtained in our tests would rate the corresponding water clearly outside recommended freshwater quality standards (6.5 < pH < 9) or limiting pH values for treatment in wastewater sewage systems (see Table 6).

Table 6. pH limit values in different local regulations.

pH Limit Values	Drinkable Water	Industrial Effluent Value for Discharge in Sewage Systems
EPA [27] (USA)	6.5 to 9	
Canada [28,29]	7 to 10.5	6–9
Switzerland [16,17]	6.8 to 8.2	6.5 to 9

Battery field failure incident reports as well as scarce pH values reported in the literature mostly report very basic contaminated water resulting from fire-fighting operations [16–18,30], although this is not always the case [31].

The basicity of the water is sometimes explained by the inner content of the cell that may contain soluble metal hydroxides. By contrast, the resulting acid fire water could be related to the interaction of the water with the acidic gases contained in the fire plume [31]. A difference in concentration in metallic species between the two tests might explain (see Table 2) the difference in pH observed. Depending on the environments in which the water will evolve (acidic or basic soils, etc.), it cannot be ruled out that these pHs are modified [32] before final pouring into aquatic ecosystems (surface of underground water resources).

4. Discussion

These tests were carried out at a small scale compared to what could occur, for example, in the event of an incident with a stationary storage container or storage warehouse. In such an event, the quantities of batteries involved, and the quantity of water used for extinction would be much higher. To estimate the orders of magnitude of water contamination values for a realistic situation (BESS container or storage warehouses), a simplistic extrapolation of the results obtained based on real incident data is proposed. In the Perles and Castelet (Ariège in France) battery stationary storage fire, which is well documented [33], and involving a stationary storage of 1500 kWh, the local authorities estimated that a volume of water of 180 m^3 was used by the firefighters, i.e., 0.12 L/Wh. This volume seems to be a good basis to extrapolate results as other feedback for other large-scale applications give similar values [34].

In the tests presented here, the volume of water used is coherent with other same-level studies [35] and, for test 1 on prismatic cells, 7 L were poured onto the 500 Wh battery (0.014 L/Wh) during test 2, and the total volume of water was 12 L (0.024 L/Wh). For the cylindrical cell, 3.9 L were poured onto the 900 Wh (0.01 L/Wh) battery. The values proposed in Table 7 correspond, for a selection of substances, to an extrapolation using a proportionality rule between the concentrations measured during the tests and the actual conditions reported during the Ariège incident (see Supplemental Material). This calculation also assumes that the normalized water flow rate (per watt-hour) does not significantly influence the mass transfer of pollutants in the run-off water.

In order to evaluate the potential environmental hazard of these wastewaters, the last column presents the "Predicted No-Effect Concentration"(PNEC) of the substance when available on the ECHA website [36]. Those values should be read with caution as they are given for a yearly average and are extracted from several sources, including industrial ones. The concentration in the wastewater was above PNEC values for all the substances studied when the data were available except for naphthalene, showing a potential environmental hazard. Two compounds show a particularly high hazardous potential: Co and EMC with concentrations, respectively, 2500 and 260 times greater than their PNEC. This means that, in a realistic scenario where two fire hoses are used to fight a fire using 1000 L/min, and the waste waters are flowing to a small river with a flow of 3 m^3/s, the concentrations of contaminants in the river are still above the PNEC for those compounds. It is also worth noting that some of the compounds' PNEC could not be found on the ECHA website but might be even more hazardous. For example, a PNEC as low as 0.0017 mg/L can be found for nickel [37] from sources other than ECHA. Another point to consider is the possible

interaction between the contaminants. To assess this, the best method would be to test the particle mix directly. Few studies of this kind are available but, Yang et al. has recently shown [8] that particles from the NMC cell thermal runaway could cause inhibition of bacterial activities in the range of 25–200 mg/L and severe acute toxicity at 100 mg/L in 5 h [8] and Quant et al. showed the acute toxicity of the runoff water [19].

Table 7. Extrapolation of the experimental results to a real application and extinguishing. The last column presents the PNEC of the compound when available on ECHA website [36].

Substance	Test 1 (Module A)	Test 2 (Module A)	Test 3 (Module B)	PNEC Freshwater
Al (mg/L)	8.7	5.9	6.2	-
Co (mg/L)	0.05	2.6	0.6	0.00106
Cu (mg/L)	0.04	0.05	0.3	0.0063
Fe (mg/L)		Test 1 (module A)	Test 2 (module A)	Test 3 (module B)
Li (mg/L)	pH	5.2	5.9	11
Mn (mg/L)	0.1	3.4	0.5	0.034
Na (mg/L)	1.8	3.3	2.2	-
Ni (mg/L)	0.4	9.8	3.3	-
P (mg/L)	23.5	22.6	0.5	-
Fluorides (mg/L)	16.6	18.3	7.8	0.89
Chlorides (mg/L)	3.9	7.3	16.9	-
EMC (mg/L)	16.1	11.8	n/a	0.062
EC (mg/L)	126.2	92.2	n/a	5.9
Naphthalene (mg/L)	0.00015	0.00056	0.00026	0.0024

5. Conclusions

In the present work, the two battery modules were triggered in thermal runaway and subsequent degassing and fire. Water was applied to mock-up firefighting operations in order to analyze the composition of the extinguishing water.

The tests presented in this paper highlight that waters used for firefighting on NMC Li-ion batteries are susceptible to containing many metals, including Ni, Mn, Co, Li and Al. Those metals are mixed with other carbonaceous species (soots, tarballs). It is also important to note that particles present in the water can be nanometric or in the form of nanostructured clusters. In addition to the solid contaminants, liquid compounds can be present, especially organic carbonates coming from the electrolyte (EC and EMC in this case) and also gaseous species such as PAH. A comparison with PNEC values showed that this water could be potentially hazardous to the environment, depending on the actual situation encountered in the case of thermal runaway propagation with a Li-ion battery-based system.

These tests also make it possible to identify some trends concerning the reaction scenario. By comparing the two extinguishing operations on the prismatic cells, one can see that when the fire is developed, the water is much more concentrated in PAH and cathode metals (Ni, Mn, Co). On the other hand, the concentrations of elements coming from the liquid electrolyte (typically Li, P, F), more easily accessible, are present in equivalent quantities. Liquid organic carbonates are preferably found in the case of degassing without ignition. These low boiling point liquids are otherwise vaporized and found mainly in the gaseous phase. The comparison of the results between the prismatic cell module and the 18,650-cell module also confirms the importance of the cell and module geometry, influencing, in particular, the mechanical strength of the system and, therefore, the confinement of the inner materials.

As large Li-ion batteries are fast spreading (in so-called Battery Energy Storage Systems, BESS, for example), and only few data on the environmental impact of fires in those systems are available, it is crucial to further develop consolidated knowledge in this field. Several directions could be suggested for future tests like developing higher level (or full

scale) testing to increase test representativity. Owing to field operational constraints in terms of emergency response following a fire, considering time between event initiation and water suppressant application as a parameter in futures studies also seems important. Other investigations worth being performed are, for instance, a detailed assessment of air, water and soil local impacts following Li-ion BESS significant incidents or in-depth environmental impact studies of key Li-ion substances like organic carbonate solvents (EC, EMC, etc.).

References

1. Giger, W. The Rhine red, the fish dead—The 1986 Schweizerhalle disaster, a retrospect and long-term impact assessment. *Environ. Sci. Pollut. Res.* **2009**, *16*, 98–111. [CrossRef] [PubMed]
2. Schwabach, A. The Sandoz spill: The failure of international law to protect the Rhine from pollution. *Ecol. LQ* **1989**, *16*, 443.
3. Zhang, H.; Duan, H.; Zuo, J.; Song, M.; Zhang, Y.; Yang, B.; Niu, Y. Characterization of post-disaster environmental management for Hazardous Materials Incidents: Lessons learnt from the Tianjin warehouse explosion, China. *J. Environ. Manag.* **2017**, *199*, 21–30. [CrossRef] [PubMed]
4. EPRI. Battery Firewater Composition and Risk Assessment. 2020. Available online: https://www.epri.com/research/products/3002020017/ (accessed on 2 February 2024).
5. *ISO TR 26368*; Environmental Damage Limitation from Fire Fighting Water Run-Off (under Revision). ISO: Geneva, Switzerland, 2012.
6. Larsson, F.; Andersson, P.; Blomqvist, P.; Lorén, A.; Mellander, B.-E. Characteristics of lithium-ion batteries during fire tests. *J. Power Sources* **2014**, *271*, 414–420. [CrossRef]
7. Feng, X.; Ouyang, M.; Liu, X.; Lu, L.; Xia, Y.; He, X. Thermal runaway mechanism of lithium ion battery for electric vehicles: A review. *Energy Storage Mater.* **2018**, *10*, 246–267. [CrossRef]
8. Yang, Y.; Fang, D.; Maleki, A.; Kohzadi, S.; Liu, Y.; Chen, Y.; Liu, R.; Gao, G.; Zhi, J. Characterization of Thermal-Runaway Particles from Lithium Nickel Manganese Cobalt Oxide Batteries and Their Biotoxicity Analysis. *ACS Appl. Energy Mater.* **2021**, *4*, 10713–10720. [CrossRef]
9. Chen, S.; Wang, Z.; Yan, W. Identification and characteristic analysis of powder ejected from a lithium ion battery during thermal runaway at elevated temperatures. *J. Hazard. Mater.* **2020**, *400*, 123169. [CrossRef]
10. Bordes, A.; Marlair, G.; Zantman, A.; Herreyre, S.; Papin, A.; Desprez, P.; Lecocq, A. New insight on the risk profile pertaining to lithium-ion batteries under thermal runaway as affected by system modularity and subsequent oxidation regime. *J. Energy Storage* **2022**, *52*, 104790. [CrossRef]
11. Mrozik, W.; Rajaeifar, M.A.; Heidrich, O.; Christensen, P. Environmental impacts, pollution sources and pathways of spent lithium-ion batteries. *Energy Environ. Sci.* **2021**, *14*, 6099–6121. [CrossRef]
12. McNamee, M.; Marlair, G.; Truchot, B.; Meacham, B.J. *Research Roadmap: Environmental Impact of Fires in the Built Environment*; Fire Protection Research Foundation: Norfolk County, MA, USA, 2020.
13. Rappsilber, T.; Yusfi, N.; Krüger, S.; Hahn, S.-K.; Fellinger, T.-P.; von Nidda, J.K.; Tschirschwitz, R. Meta-analysis of heat release and smoke gas emission during thermal runaway of lithium-ion batteries. *J. Energy Storage* **2023**, *60*, 106579. [CrossRef]
14. Vilic, A. *Environmental Risk Assessment of Fire-Water Runoff from Vehicle Fire-Development of a Predictive Model Intended for the Fire-Rescue Service*; Fire Protection Research Foundation: Norfolk County, MA, USA, 2019.
15. Noiton, D.; Fowles, J.; Davies, H. The ecotoxity of Fire Water Run-off, Part II: Analytical Results, New Zealand Fire Service Commission Research Report Number 18. 2001. ISBN 0-908920-61. Available online: https://www.researchgate.net/publication/272508692_Fire_Research_The_Ecotoxicity_of_Fire-Water_Runoff_Part_II_Analytical_Results_ESR#fullTextFileContent (accessed on 3 March 2024).

16. EMPA. Minimization of Fire Risks from Electric Vehicles in Underground Traffic Infrastructures. 2018. Available online: https://plus.empa.ch/images/2020-08-17_Brandversuch-Elektroauto/AGT_2018_006_EMob_RiskMin_Undergr_Infrastr_Final_Report_V1.0.pdf (accessed on 2 February 2024).

17. Held, M.; Tuchschmid, M.; Zennegg, M.; Figi, R.; Schreiner, C.; Mellert, L.D.; Welte, U.; Kompatscher, M.; Hermann, M.; Nachef, L. Thermal runaway and fire of electric vehicle lithium-ion battery and contamination of infrastructure facility. *Renew. Sustain. Energy Rev.* **2022**, *165*, 112474. [CrossRef]

18. RIVM. Risico's Van Rook Door Branden Van Li-Ionbatterijen. 2021. Available online: https://www.rivm.nl/bibliotheek/rapporten/2021-0019.pdf (accessed on 2 February 2024).

19. Quant, M.; Willstrand, O.; Mallin, T.; Hynynen, J. Ecotoxicity Evaluation of Fire-Extinguishing Water from Large-Scale Battery and Battery Electric Vehicle Fire Tests. *Environ. Sci. Technol.* **2023**, *57*, 4821–4830. [CrossRef] [PubMed]

20. Zhang, Y.; Wang, H.; Li, W.; Li, C.; Ouyang, M. Size distribution and elemental composition of vent particles from abused prismatic Ni-rich automotive lithium-ion batteries. *J. Energy Storage* **2019**, *26*, 100991. [CrossRef]

21. Dyer, J.A.; Scrivner, N.C.; Dentel, S.K. A practical guide for determining the solubility of metal hydroxides and oxides in water. *Environ. Prog.* **1998**, *17*, 1–8. [CrossRef]

22. Winberry, W.T.; Murphy, N.T.; Riggan, R. *Compendium of Methods for the Determination of Toxic Organic Compounds in Ambient Air*; EPA, National Service Center for Environmental Publications: Washington, DC, USA, 1988.

23. Geiser, M.; Kreyling, W.G. Deposition and biokinetics of inhaled nanoparticles. *Part. Fibre Toxicol.* **2010**, *7*, 2. [CrossRef] [PubMed]

24. Wang, X.; Xie, H.; Wang, P.; Yin, H. Nanoparticles in plants: Uptake, transport and physiological activity in leaf and root. *Materials* **2023**, *16*, 3097. [CrossRef] [PubMed]

25. Rivero Arze, A.; Mouneyrac, C.; Chatel, A.; Manier, N. Comparison of uptake and elimination kinetics of metallic oxide nanomaterials on the freshwater microcrustacean Daphnia magna. *Nanotoxicology* **2021**, *15*, 1168–1179. [CrossRef]

26. Rivero Arze, A.; Manier, N.; Chatel, A.; Mouneyrac, C. Characterization of the nano–bio interaction between metallic oxide nanomaterials and freshwater microalgae using flow cytometry. *Nanotoxicology* **2020**, *14*, 1082–1095. [CrossRef] [PubMed]

27. Available online: https://www.epa.gov/sdwa/drinking-water-regulations-and-contaminants (accessed on 2 February 2024).

28. Available online: https://www.canada.ca/fr/sante-canada/services/publications/vie-saine/recommandations-pour-qualite-eau-potable-canada-chlore-document-technique/page-3-recommandations-pour-qualite-eau-potable-canada-chlore-document-technique.html (accessed on 2 February 2024).

29. Ottawa City Service. Guide Discharging Waste Water Ind. *Facilities.* 2011. Available online: https://nchca.ca/wp-content/uploads/2017/06/Sewer-Use-Program_English_2011.pdf (accessed on 22 March 2024).

30. LCPP. Étude de l'Impact de Feux de Véhicules Electriques (RENAULT) sur les Intervenants des Services de Secours. 2015. Available online: http://iuv.sdis86.net/wp-content/uploads/2015/09/Rapport-LCPP-brulages-vehicules-electriques-Renault.pdf (accessed on 2 February 2024).

31. Alberto Project. Available online: https://alberoprojekt.de/index_htm_files/WP%201.4%20Contamination%20of%20extinguishing%20water%20after%20fires%20of%20Li-Ion%20Batteries.pdf (accessed on 2 February 2024).

32. Merseyside Fire & Rescue Service. SIGNIFICANT INCIDENT REPORT—018965—15092020—Orsted BESS, Carnegie Road, Liverpool, L137HY. 2021. Available online: https://planningregister.cherwell.gov.uk/Document/Download?module=PLA&recordNumber=154109&planId=1951104&imageId=30&isPlan=False&fileName=Appendix%202%20%20-%20Liverpool%20BESS%20Significant%20Investigation%20Report%20(1).pdf (accessed on 28 March 2024).

33. BEA-RI. Rapport d'Enquête Technique sur l'Incendie au Sein du Poste de Transformation RTE. de Perles et Castelet (09). 2021. Available online: https://www.igedd.developpement-durable.gouv.fr/IMG/pdf/rapportperlesvdif_cle286783.pdf (accessed on 2 February 2024).

34. Tesla. Model 3 Emergency Response Guide. 2018. Available online: https://www.tesla.com/sites/default/files/downloads/2017_Model_3_Emergency_Response_Guide_en.pdf (accessed on 2 February 2024).

35. Zhang, L.; Duan, Q.; Liu, Y.; Xu, J.; Sun, J.; Xiao, H.; Wang, Q. Experimental investigation of water spray on suppressing lithium-ion battery fires. *Fire Saf. J.* **2021**, *120*, 103117. [CrossRef]

36. Available online: https://echa.europa.eu/fr/home (accessed on 2 February 2024).

37. Available online: https://substances.ineris.fr/fr/substance/1301/3 (accessed on 2 February 2024).